Received: 30 July 2021 | Revised: 9 December 2021 | Accepted: 21 December 2021

DOI: 10.1002/dvdy.454

RESEARCH ARTICLE

Developmental Dynamics WILEY

Investigating the effects of compound paralogous EPHB receptor mutations on mouse facial development

Sarah T. Mincer[1] | **Terren K. Niethamer**[2,3,4,5] | **Teng Teng**[2,3,4,5] | **Jeffrey O. Bush**[2,3,4,5] | **Christopher J. Percival**[6]

[1]Interdepartmental Doctoral Program in Anthropological Sciences, Stony Brook University, Stony Brook, New York, USA

[2]Program in Craniofacial Biology, University of California San Francisco, San Francisco, California, USA

[3]Department of Cell and Tissue Biology, University of California San Francisco, San Francisco, California, USA

[4]Institute for Human Genetics, University of California San Francisco, San Francisco, California, USA

[5]Biomedical Sciences Graduate Program, University of California San Francisco, San Francisco, California, USA

[6]Department of Anthropology, Stony Brook University, Stony Brook, New York, USA

Correspondence
Jeffrey O. Bush, Department of Cell and Tissue Biology, University of California, San Francisco 513 Parnassus Avenue, HSE San Francisco, CA 94143, USA.
Email: jeffrey.bush@ucsf.edu

Christopher J. Percival, Department of Anthropology, Stony Brook University Stony Brook, NY 11794, USA.
Email: christopher.percival@stonybrook.edu

Funding information
National Institute of Dental and Craniofacial Research, Grant/Award Number: R01-DE023337; Stony Brook University, Grant/Award Number: Startup Funds

Abstract

Background: Variation in facial shape may arise from the combinatorial or overlapping actions of paralogous genes. Given its many members, and overlapping expression and functions, the EPH receptor family is a compelling candidate source of craniofacial morphological variation. We performed a detailed morphometric analysis of an allelic series of E14.5 *Ephb1-3* receptor mutants to determine the effect of each paralogous receptor gene on craniofacial morphology.

Results: We found that *Ephb1*, *Ephb2*, and *Ephb3* genotypes significantly influenced facial shape, but *Ephb1* effects were weaker than *Ephb2* and *Ephb3* effects. $Ephb2^{-/-}$ and $Ephb3^{-/-}$ mutations affected similar aspects of facial morphology, but $Ephb3^{-/-}$ mutants had additional facial shape effects. Craniofacial differences across the allelic series were largely consistent with predicted additive genetic effects. However, we identified a potentially important nonadditive effect where *Ephb1* mutants displayed different morphologies depending on the combination of other *Ephb* paralogs present, where $Ephb1^{+/-}$, $Ephb1^{-/-}$, and $Ephb1^{-/-}$; $Ephb3^{-/-}$ mutants exhibited a consistent deviation from their predicted facial shapes.

Conclusions: This study provides a detailed assessment of the effects of *Ephb* receptor gene paralogs on E14.5 mouse facial morphology and demonstrates how the loss of specific receptors contributes to facial dysmorphology.

KEYWORDS

additive genetic effects, allometry, craniofacial, *Efnb1*, EPHRIN-B1, morphological variation

1 | INTRODUCTION

Paralagous genes arise during gene duplication events, and the resulting gene copies can retain functionally redundant effects or diverge and take on different developmental functions.[1-6] Paralogs expressed in overlapping developmental domains often exhibit functional interaction, resulting in either additive or nonadditive genetic

effects. Additive genetic interaction effects occur in a linear fashion where the combined effect of two alleles (eg, mutations) is simply the sum of the effects of each individual allele. Additive genetic interactions between disease mutations in genes with parallel functional effects should lead to increased severity of the resulting phenotype. In contrast, nonadditive genetic effects are present when phenotypic effects cannot be simply summed, and genes instead interact in different ways such as epistatic dominance effects between mutations and minimum threshold effects whereby homozygosity is required for dysmorphology to occur. A similar nonadditive threshold effect may occur if compound loss-of-function mutations in two redundant paralogs produces dysmorphology, but homozygous loss of function of only one of the paralogs is indistinguishable from control specimens.

Paralogous genes that take on novel and divergent developmental functions provide a critical basis for generating morphological variation and evolutionary change.[2-4,7,8] For example, duplication of *Hox* genes has contributed to the evolution of the vertebrate body plan, allowing for diversification and regional specialization of the vertebrate axial skeleton.[2,4,9-12] Paralogs that instead retain all or some of their original function may provide protection from deleterious effects of mutations in one paralog or may interact and be dependent on each other for normal function.[6-8,13] Quantifying and comparing the specific additive and nonadditive genetic effects of paralogous genes on craniofacial shape would improve our understanding of the individual and combined impacts of those genes during typical development of facial structures. Further, understanding the developmental functions of paralogs can aid in identifying the role that specific mutations play in producing dysmorphologies associated with certain diseases.

For example, a breakdown in normal signaling between the EPHRIN-B1 ligand and its associated receptors can result in serious craniofacial dysmorphology.[14-18] *EFNB1* encodes EPHRIN-B1, a transmembrane protein and signaling partner of multiple EPHB receptors.[15,17-20] Signaling between EPHB receptors and EPHRIN signaling partners is integral to the development of various tissues, including the central nervous system, and plays a role in tissue boundary formation, cell migration, and neurogenesis.[20-26] Mutations in the *EFNB1* gene cause Craniofrontonasal syndrome (CFNS, OMIM #304110), an X-linked, developmental disorder associated with craniofacial dysmorphologies such as increased distance between the orbits (ie, hypertelorism), irregular fusion of the cranial sutures (ie, craniosynostosis), craniofacial asymmetry, and a grooved or bifid nasal tip.[15,17,27]

While the EPHRIN-B1 protein is encoded by a single gene, it binds with different affinities to multiple EPHB receptors that are encoded by paralogous genes, which have both overlapping and distinct biological functions.[18,19,28] *Eph* and *Ephrin* genes are widely expressed throughout the body, with EPHB receptors having prominent expression in the central nervous system and craniofacial complex.[14,18,20,29,30] Overlapping expression of *Eph* receptor genes in the craniofacial complex during early development may allow for some receptors to compensate for loss of others that have similar expression patterns and ligand-binding affinities.[28] Further, EPHB1-3 also have different binding affinities to EPHRIN-B1, and to other EPHRIN signaling partners, leading to both distinct and overlapping effects during development, which are likely required to produce normal facial shape. For example, *Ephb1-3* are all expressed during palatal development but have differing functions.[14,18,28,31,32] While *Ephb1* expression is widespread but weak throughout the palatal shelves, *Ephb2* and *Ephb3* are both critical for normal palate development.[14,28] Mice with loss of both *Ephb2* and *Ephb3* have high instances of cleft palate, while those with loss of either *Ephb2* or *Ephb3* appear to have normal palate cell proliferation and adhesion, suggesting functional redundancy of these receptors in the palatal shelves.[31] Quantitative assessment of an allelic series of *Ephb1-3* compound mutants revealed different patterns of expression in the brain, frontonasal prominence, and secondary palate.[14] *Ephb1* has the weakest expression throughout the frontonasal mesenchyme with a minor impact on facial development while *Ephb2* and *Ephb3* mutant genotypes lead to more severe dysmorphology and are more critical for normal facial development.[14,28] Thus, although these paralogous receptors are all major binding partners of EPHRIN-B1, they have unequal influences on craniofacial development.

A deeper understanding of the combinatorial influence of EPHB1-3 receptor paralogs on the development of facial morphology can improve our understanding of how changes to specific EPH/EPHRIN signaling factors might contribute to the evolution of the mammalian craniofacial complex. EPH/EPHRIN signaling is known to contribute to the early development of tissues in the head, face, and brain. Therefore, the duplication and divergence of specific EPHB receptor functions may serve as a substrate for evolutionary change in relevant developmental processes.[5,18,19,28] For example, EPHB1-3 have different patterns of expression and may function in distinct or overlapping tissues in the face, and combinatorial functions of receptors may produce novel morphologies where they overlap.[14,20,29] In fact, EPH receptors and their EPHRIN binding partners diversified at different points in the evolutionary history of vertebrates, and duplication of EPH receptors may have permitted subtle variations in how and where they function during

vertebrate development, allowing for more complex processes and interactions.[5] However, a more detailed analysis of the morphological variation among *Ephb1-3* mutant genotypes is needed to describe and quantify the specific craniofacial phenotype associated with each receptor gene independently, and how they interact to produce normal facial morphology. This may ultimately help identify how they have diversified during mammalian evolution, potentially providing a platform for evolutionary change.

Here, we perform an in-depth morphometric analysis of an allelic series of E14.5 *Ephb1-3* compound genotype mutants, providing a thorough assessment of each receptor's contribution to craniofacial morphogenesis. We first determine the relative influence of homozygous loss-of-function mutations of individual *Ephb* receptor genes on E14.5 craniofacial shape and then document the shape changes associated with loss of each receptor gene to determine whether receptors affect overlapping or distinct regions of the face. To gain a deeper understanding of the specific effects of the role of each receptor, both on its own and with compound loss, we then examine whether the overall morphological effect of multiple *Ephb* mutant alleles can be predicted as the additive combination of individual mutant allele effects. In this context, a purely additive genetic model predicts that facial dysmorphology of an *Ephb* homozygous mutant is simply twice as severe as the facial dysmorphology of a heterozygous mutant for a given *Ephb* gene. Similarly, an additive genetic model predicts that the combined loss-of-function effects for multiple *Ephb* receptor genes are the sum total of individual receptor loss-of-function effects. If these predictions are not supported, this indicates the existence of nonadditive genetic effects between receptor alleles during facial morphogenesis, such as dominance of one receptor gene over another, or minimum threshold effects where the loss of multiple functionally redundant receptors are required to produce dysmorphology. Finally, we assess the effects of different *Ephb* gene mutations on craniofacial size (in addition to shape) to examine the potential allometric link between overall facial growth and the production of facial dysmorphology.

Our detailed analysis of the particular dysmorphologies present across this *Ephb* allelic series pinpoints the specific roles of paralogous EPHB receptors within the EPHRIN-B1 signaling pathway that are critical to normal facial development. Quantifying the nature of genetic interactions between *Ephb* mutations allows us to identify possible epistatic interactions between EPHB receptors that are known to interact with an overlapping set of the same EPHRIN signaling partners. This will improve our understanding of the combinatorial effect of allelic variation on normal processes of facial development and how novel mutations could contribute to CFNS-like dysmorphology.

2 | RESULTS

2.1 | Procrustes ANOVA

To quantify the proportion of facial shape variation attributed to each *Ephb* receptor gene mutation and to facial size, as well as potential interaction effects between receptor genotypes, we ran two separate Procrustes ANOVA models: an additive model (Supplementary Table S1) and an interaction model (Table 1). Factors in the interaction model are the same as in the additive model, but with additional terms that represent multiplicative interaction between two or three receptors. Thus, results of the additive model represent a subset of the interaction model where the additive factors are also found within the interaction model. Our Procrustes shape analyses were performed using facial landmarks (Figure 1) that have been scaled using a generalized Procrustes superimposition (GPA) and therefore provide comparisons of the size of morphological features relative to other features and not the original measured size of those features.

The results of the Procrustes ANOVA with interaction effects indicated that facial size, as well as mutation of any one of the three analyzed *Ephb* genes, contributed significantly to facial shape (Table 1: size [$P < .001$], *Ephb1* [$P = .013$], *Ephb2* [$P < .001$], and *Ephb3* [$P < .001$]). Facial size explained 28.4% of facial shape variation in this sample of E14.5 mice (based on Rsq), while *Ephb1*, *Ephb2*, and *Ephb3* genotypes explained 1.2%, 6.8%, and 11.1%, respectively. Effect sizes (denoted by Z-scores) also indicated that facial size had the strongest influence on facial morphology ($Z = 6.98$), followed by *Ephb3* genotype ($Z = 6.73$) and *Ephb2* genotype ($Z = 5.65$). While interactions between each combination of two *Ephb* genotypes were not significant, the interaction between combinations of all three *Ephb* receptor genes was significant ($P = .013$) and explained approximately 1.0% of facial variation. This result indicates nonadditive effects of different combinations of *Ephb1-3* genotypes. In other words, although we found significant additive effects on facial shape for single-gene mutant alleles (ie, *Ephb1*, *Ephb2*, or *Ephb3*) as well as a nonadditive interaction effect when all three *Ephb* receptor genotypes were considered at once, there was not a consistent interaction effect between pairs of *Ephb* genes. This indicates either a lack of genotype effects of different pairwise combinations of *Ephb* gene mutations or that pairwise interaction effects were not consistent across the full allelic series.

	df	SS	MS	*Rsq*	*F*	*Z*	*P*
Facial size	1	0.048	0.048	0.284	64.9	6.98	.001**
Ephb1	1	0.002	0.002	0.012	2.82	2.33	.013*
Ephb2	1	0.011	0.011	0.068	15.5	5.65	.001**
Ephb3	1	0.019	0.019	0.111	25.5	6.73	.001**
Ephb1 × *Ephb2*	1	0.001	0.001	0.007	1.67	1.40	.075
Ephb1 × *Ephb3*	1	0.001	0.001	0.005	1.08	0.46	.336
Ephb2 × *Ephb3*	1	0.001	0.001	0.006	1.29	0.77	.222
Ephb1 × *Ephb2* × *Ephb3*	1	0.002	0.002	0.010	2.35	2.24	.013*

TABLE 1 Results of Procrustes ANOVA testing the interaction effects of *Ephb* genotype and facial size on craniofacial morphology

Note: 3D symmetrized landmark coordinates as the response variable, and size (numeric: centroid size) and genotype (separate numeric factors: 0, 1, 2 null alleles for *Ephb1*, *Ephb2*, and *Ephb3*) as independent variables. For each factor: df is the degrees of freedom, SS is the sum-of-squared Procrustes distances, MS is the mean sum-of-squares (SS/df), Rsq is the estḥimate of how much facial shape variation is attributable to each factor, F is the test statistic comparing the MS to the amount of variation within groups, Z is the effect size (associated with F), and *P* is the probability of getting an F score higher than this factor's *F* score by random chance alone.

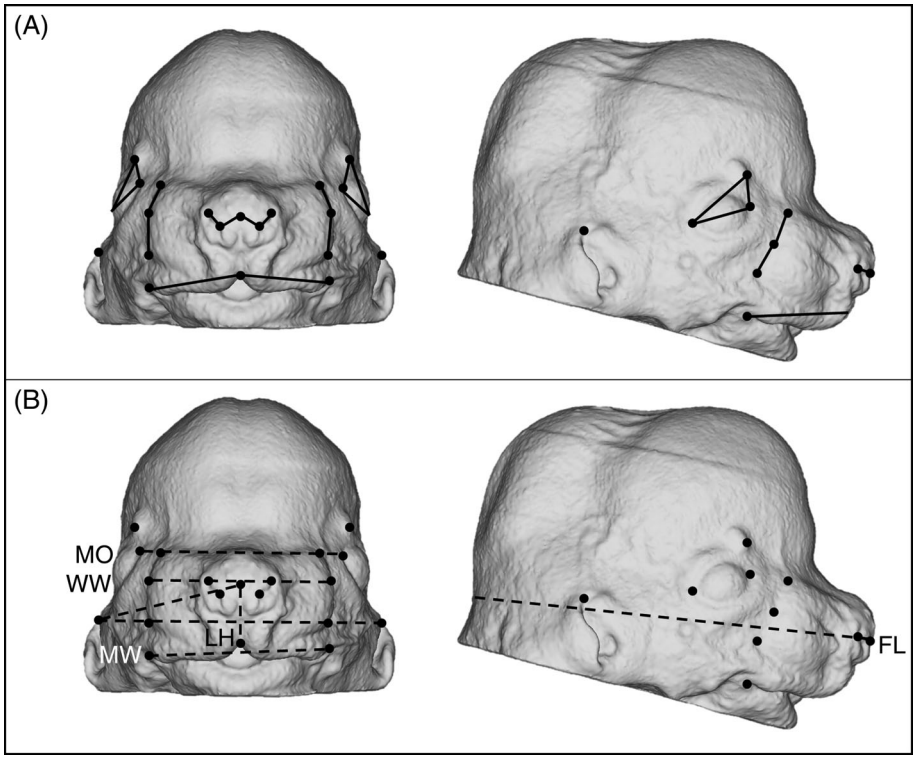

FIGURE 1 Landmarks taken on E14.5 mice placed on a 3D surface representation of μCT images. Brief landmark descriptions included in Supplementary Table S5, for full description of landmarks taken, see Niethamer et al.[14] (A) Solid connecting reference lines included to aid in morphological interpretations. (B) Dashed lines representing linear facial size measurements taken between raw landmark coordinates for size comparison between genotypes. Linear measurements include facial length (FL), medial orbit width (MO), upper lip height (LH), mouth width (MW) and mid whisker width (WW)

2.2 | Predicted facial shape differences

We predicted average facial landmark coordinates for each genotype in the allelic series using the fitted values and associated covariates from both the additive and interaction Procrustes ANOVA models (Figure 2). Predicting facial landmark coordinates from an ANOVA model is like predicting values from a linear regression where the influence of all size and genotype factors in the model are considered, across the entire allelic series. Utilizing facial shape predictions rather than more simple morphometric approaches allowed us to visualize and compare general trends in *Ephb* mutation shape effects across the entire sample and estimate the effects of and interactions between specific *Ephb* receptor genes based on effects measured across the whole series of 27 genotypes.

To illustrate the predicted additive genotype effects from our model, we generated plots of shape differences between select homozygous mutant genotypes and controls represented as vectors connecting the predicted facial shape coordinates of controls to mutants (Figure 2).

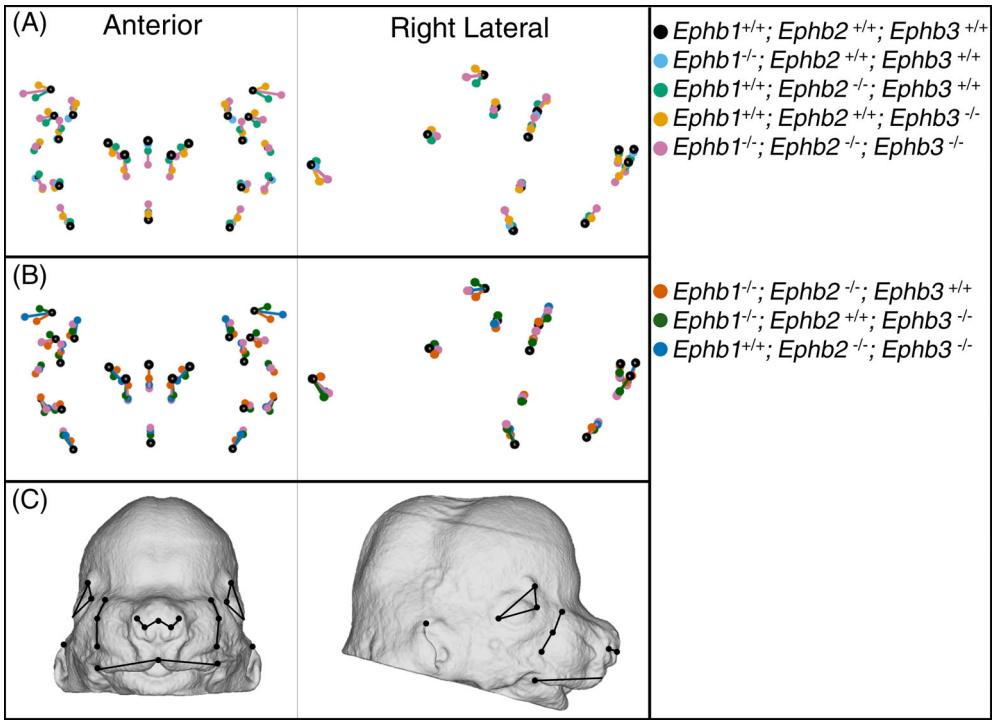

FIGURE 2 Vectors connecting the predicted genotype specific shape coordinates for select genotypes in anterior and lateral views. Black circles represent control specimens (*Ephb1*$^{+/+}$; *Ephb2*$^{+/+}$; *Ephb3*$^{+/+}$), each colored dot and matching colored vector represent the shape difference from the mean control shape to the mean shape for (A) homozygous single nulls, (B) homozygous double nulls, and (A,B) homozygous triple nulls. Vectors are magnified ×3 to better see shape differences between genotypes. (C) Landmarks and solid connecting reference lines represented on ectodermal surface included to aid in morphological interpretations

We measured the strength of shape differences between genotypes using Procrustes distances to determine whether specific mutant genotype facial shapes were significantly different than control facial shapes (Supplementary Table S2). In the most extreme comparison, our model indicates that *Ephb1*$^{-/-}$; *Ephb2*$^{-/-}$; *Ephb3*$^{-/-}$ mutant mice exhibited more inferiorly placed nostrils and superiorly placed upper lip margin (suggesting an overall shorter philtrum and upper lip), laterally placed orbits (hypertelorism), superiorly placed whisker margins (suggesting increased whisker region height), and antero-inferiorly placed ear pinnae (suggesting overall shorter faces) compared to control specimens (Figure 2).

Our models predicted different effects on facial shape for different homozygous mutant genotypes. *Ephb1*$^{-/-}$ effects are minor, leading to a predicted facial shape that is close to control shape (Figure 2A). The predicted shape for *Ephb2*$^{-/-}$ included nostrils that are more narrowly spaced, and orbits that are more laterally and inferiorly placed than other genotypes (Figure 2A). *Ephb3*$^{-/-}$ faces were predicted by the model to be intermediate in shape between controls and triple homozygous mutant mice (*Ephb1*$^{-/-}$; *Ephb2*$^{-/-}$; *Ephb3*$^{-/-}$) for most landmarks, including the nostrils, whisker margins, and mouth. *Ephb3* homozygous mutation was also predicted to have a greater effect on the position of the ear pinnae than other single homozygous gene mutations (Figure 2A).

Ephb1$^{-/-}$; *Ephb2*$^{-/-}$ mutants were predicted to be closest in shape to *Ephb2*$^{-/-}$ mutants but exhibit more inferiorly placed nostrils and superiorly placed upper lip, indicative of a shortened philtrum and upper lip (Figure 2B). *Ephb1*$^{-/-}$; *Ephb3*$^{-/-}$ mutants were similar in shape to *Ephb3*$^{-/-}$ mutants, with both genotypes displaying hypertelorism, and a shortened philtrum and upper lip (Figure 2B). *Ephb1*$^{-/-}$; *Ephb3*$^{-/-}$ mutants also exhibited a similar displacement of the ear pinnae seen in *Ephb3*$^{-/-}$ mutants. The predicted shape for *Ephb2*$^{-/-}$; *Ephb3*$^{-/-}$ mutants was closest to triple homozygous mutants and is notably more severe than either *Ephb2*$^{-/-}$ or *Ephb3*$^{-/-}$ single mutants (Figure 2B). This result indicated a severe compound effect with homozygous loss of both *Ephb2* and *Ephb3* receptor genes. Based on a lack of significant interaction effect between these two genes in the interaction Procrustes ANOVA model (Table 1), we believe that this predicted compound effect is additive in nature. Similar to the predicted shape for triple homozygous mutants, *Ephb2*$^{-/-}$; *Ephb3*$^{-/-}$ embryos exhibited more narrowly spaced nostrils, shorter upper lip margins, more laterally placed orbits, more superiorly placed

whisker margins, and more antero-inferiorly placed ear pinnae compared to control specimens and single gene homozygous mutants.

In addition, facial shapes predicted by our statistical models suggested that while homozygous loss of *Ephb1* on its own had minimal effects on facial morphology, homozygous loss of either *Ephb2* or *Ephb3* led to consistent and notable facial shape effects in partially overlapping regions of the face. For example, both *Ephb2*$^{-/-}$ and *Ephb3*$^{-/-}$ mutants were predicted by the models to exhibit hypertelorism, but only *Ephb3*$^{-/-}$ mutants were predicted to have displaced ear pinnae and a moderately shortened relative upper lip height. Further, homozygous loss of *Ephb2* and *Ephb3* together was predicted to have notably more severe dysmorphologies than loss of a single receptor. However, homozygous loss of *Ephb1* in combination with the other receptors had a minor or no additional predicted effect on facial morphology.

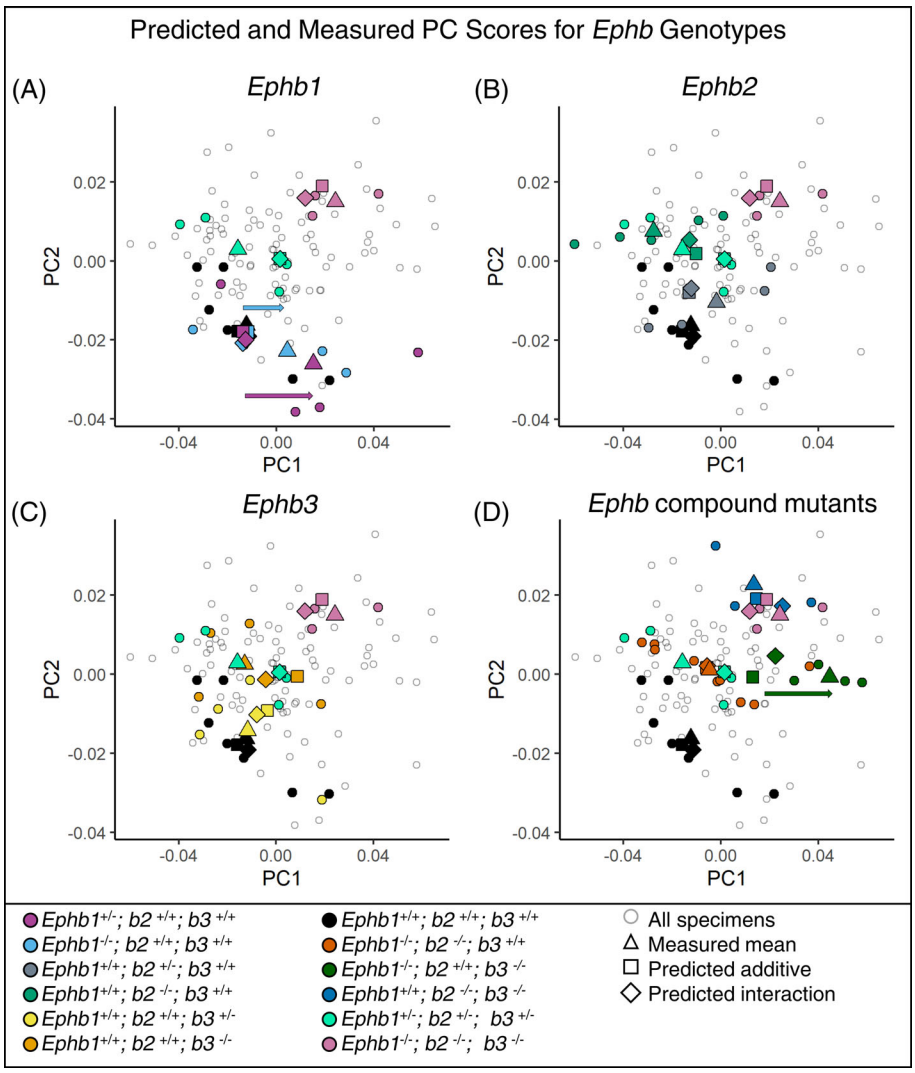

FIGURE 3 PC2-PC1 scores of all specimens included in this study (smaller gray circles), with PC scores of *Ephb* genotypes indicated by smaller, colored circles. Measured and predicted mean PC scores for each genotype are denoted by corresponding larger shapes: Measured mean values indicated by triangles, predicted facial shape coordinates from an additive model indicated by squares, and predicted facial shape coordinates from an interaction model indicated by diamonds. Genotypes denoted by color. Colored arrows in panels (A) and (D) highlight *Ephb1* PC1 shifts described in results. (A) *Ephb1* single gene heterozygotes (*Ephb1*$^{+/-}$; *Ephb2*$^{+/+}$; *Ephb3*$^{+/+}$) and *Ephb1* single gene homozygotes (*Ephb1*$^{-/-}$; *Ephb2*$^{+/+}$; *Ephb3*$^{+/+}$), (B) *Ephb2* single gene heterozygotes (*Ephb1*$^{+/+}$; *Ephb2*$^{+/-}$; *Ephb3*$^{+/+}$) and *Ephb2* single gene homozygotes (*Ephb1*$^{+/+}$; *Ephb2*$^{-/-}$; *Ephb3*$^{+/+}$), (C) *Ephb3* single gene heterozygotes (*Ephb1*$^{+/+}$; *Ephb2*$^{+/+}$; *Ephb3*$^{+/-}$) and *Ephb3* single-gene homozygotes (*Ephb1*$^{+/+}$; *Ephb2*$^{+/+}$; *Ephb3*$^{-/-}$), (D) *Ephb1/Ephb2* double-gene homozygotes (*Ephb1*$^{-/-}$; *Ephb2*$^{-/-}$; *Ephb3*$^{+/+}$), *Ephb1/Ephb3* double-gene homozygotes (*Ephb1*$^{-/-}$; *Ephb2*$^{+/+}$; *Ephb3*$^{-/-}$), *Ephb2/Ephb3* double-gene homozygotes (*Ephb1*$^{+/+}$; *Ephb2*$^{-/-}$; *Ephb3*$^{-/-}$). Controls (*Ephb1*$^{+/+}$; *Ephb2*$^{+/+}$; *Ephb3*$^{+/+}$), triple gene heterozygotes (*Ephb1*$^{+/-}$; *Ephb2*$^{+/-}$; *Ephb3*$^{+/-}$), and triple gene homozygotes (*Ephb1*$^{-/-}$; *Ephb2*$^{-/-}$; *Ephb3*$^{-/-}$) included in all panels for comparison

Specifically, *Ephb1*$^{-/-}$; *Ephb2*$^{-/-}$ and *Ephb1*$^{-/-}$; *Ephb3*$^{-/-}$ mutants shared similar predicted shape dysmorphology with *Ephb2*$^{-/-}$ and *Ephb3*$^{-/-}$ mutants, respectively. In addition, *Ephb2*$^{-/-}$; *Ephb3*$^{-/-}$ mutants had dysmorphology similar to *Ephb1*$^{-/-}$; *Ephb2*$^{-/-}$; *Ephb3*$^{-/-}$ mutants. In summary, our additive genetic model predicted a strong facial shape effect associated with *Ephb2*$^{-/-}$ and *Ephb3*$^{-/-}$ gene mutations and a stronger effect in *Ephb2*$^{-/-}$; *Ephb3*$^{-/-}$ mutants, suggesting that *Ephb2* and *Ephb3* are the principal receptor genes contributing to normal craniofacial development.

2.3 | Predicted vs measured PC scores

We first calculated principal components (PCs) scores using the measured facial shape of every specimen in our allelic series and plotted these scores for each measured specimen across the sample. Next, we calculated the mean shape of each genotype based on measured specimen facial shape and plotted these alongside all of the specimen PC scores. Then, we estimated the PC scores of each genotype's predicted facial shape based on both additive and interaction linear models and plotted these scores alongside the measured specimen PC scores. This comparison of measured and predicted facial shapes allowed us to determine how well our statistical models represented the measured shape of each genotype (Figure 3). Here, we describe and compare the predicted scores and measured scores to highlight how our measured facial shapes diverged from model predictions. A systematic difference between a genotype's measured facial shape (calculated from landmark coordinates) and that genotype's predicted facial shape (predicted from the models) suggests a genotype-specific nonadditive effect on facial development that is not explained by our additive or interaction linear models (ie, the Procrustes ANOVA models). These results were derived from Procrustes superimposed landmark coordinates and represent differences in facial shape rather than differences in facial size. Therefore, all descriptions of facial shape related to PC scores refer to the size and position of morphological features relative to one another and not the measured size of those features, which was analyzed separately.

Principal component 1 (PC1) captured approximately 46% of facial shape variation across all measured samples (Supplementary Table S3) and was associated with variation in relative facial width and length across our sample. Specimens with larger PC1 values had rostro-caudally shorter and mediolaterally wider faces than specimens with smaller PC1 values. PC2 captured approximately 14% of measured facial variation (Supplementary Table S3) and was associated with variation in relative facial height and orbit width. Specimens with larger PC2 values had mediolaterally wider space between the orbits and dorsoventrally shorter faces than specimens with smaller PC2 values.

Predicted shapes for *Ephb1*$^{+/+}$; *Ephb2*$^{+/+}$; *Ephb3*$^{+/+}$ and for *Ephb1*; *Ephb2*; *Ephb3* triple heterozygous and homozygous mutants were separated along both the first and second PC axes (Figure 3A-D). Control specimens had the smallest predicted values for PC1 and PC2, *Ephb1*$^{+/-}$; *Ephb2*$^{+/-}$; *Ephb3*$^{+/-}$ compound heterozygous mutants were intermediate, and *Ephb1*$^{-/-}$; *Ephb2*$^{-/-}$; *Ephb3*$^{-/-}$ compound homozygous mutants had the largest predicted values for PC1 and PC2. *Ephb1*$^{-/-}$; *Ephb2*$^{-/-}$; *Ephb3*$^{-/-}$ mutants had the mediolaterally widest and rostro-caudally shortest faces of all specimens included in the sample. Measured scores for both controls and *Ephb1*$^{-/-}$; *Ephb2*$^{-/-}$; *Ephb3*$^{-/-}$ mutants plotted closely with predicted scores, while *Ephb1*$^{+/-}$; *Ephb2*$^{+/-}$; *Ephb3*$^{+/-}$ compound heterozygous embryos showed a smaller mean PC1 score than predicted.

Predicted scores for *Ephb1*$^{+/-}$ *and Ephb1*$^{-/-}$ mutants plotted closely with controls (Figure 3A). This suggests that across the entire sample, *Ephb1* is predicted to have very minor effects on facial shape. However, the measured specimen means for *Ephb1*$^{+/-}$ and *Ephb1*$^{-/-}$ PC1 scores were larger than the predicted PC scores for these genotypes (signified by colored arrows in Figure 3A). The unexpected position of measured means towards the positive end of PC1 suggests a genetic effect of *Ephb1* on facial shape that was not captured by our additive or interaction Procrustes ANOVA models. If this genotype effect is significant, it resulted in a higher PC1 score, which is associated with a relatively wider face and shorter head. This is notably different than the effects of *Ephb2* and *Ephb3* genotype mutations, which resulted in simultaneously increased PC1 and PC2 scores within our analysis.

The predicted means for *Ephb2*$^{+/-}$ and *Ephb2*$^{-/-}$ mutants were intermediate between controls and homozygous triple mutants for PC1 and PC2, with the predicted mean for *Ephb2*$^{-/-}$ mutants plotting approximately twice as far along PC2 as *Ephb2*$^{+/-}$ mutants (Figure 3B). Similarly, the predicted means for *Ephb3*$^{+/-}$ and *Ephb3*$^{-/-}$ mutants were also intermediate between controls and triple homozygous mutants for PC1 and PC2 (Figure 3C). In essence, *Ephb2* or *Ephb3* homozygous mutants were predicted to display dysmorphology that was approximately twice as severe as the dysmorphology for heterozygous mutants for the same receptor. Measured means for *Ephb2*$^{+/-}$ and *Ephb2*$^{-/-}$ mutants plotted closely with their predicted means (with

minor shifts along PC1) (Figure 3B). Measured means for *Ephb3*$^{+/-}$ and *Ephb3*$^{-/-}$ mutants also plotted closely with their predicted means, although the measured mean for *Ephb3*$^{+/-}$ mutants was also close to the measured mean for controls (Figure 3C). Overall, the shape effects of *Ephb2* and *Ephb3* mutations appeared to be predicted well by our additive model, indicating that *Ephb2* and *Ephb3* genotypic effects appear largely additive in nature. However, because measured *Ephb2*$^{+/-}$ and *Ephb3*$^{+/-}$ mutant individuals also overlapped with measured controls (and the measured *Ephb3*$^{+/-}$ mean overlaps with the measured control mean), it is possible that heterozygous mutants are actually indistinguishable from control specimens, which would mean that homozygous loss of a single receptor is necessary to produce dysmorphology in the absence of other receptor mutations.

Predicted means for *Ephb1*$^{-/-}$; *Ephb2*$^{-/-}$ and *Ephb1*$^{-/-}$; *Ephb3*$^{-/-}$ mutants plotted near the predicted means for *Ephb1*$^{+/-}$; *Ephb2*$^{+/-}$; *Ephb3*$^{+/-}$ mutants, with *Ephb1*$^{-/-}$; *Ephb3*$^{-/-}$ having slightly larger predicted PC1 values (Figure 3D). In contrast, the predicted mean shape for *Ephb2*$^{-/-}$; *Ephb3*$^{-/-}$ mutants plotted closely to the mean shape for *Ephb1*$^{-/-}$; *Ephb2*$^{-/-}$; *Ephb3*$^{-/-}$ mutants. The measured mean for *Ephb1*$^{-/-}$; *Ephb2*$^{-/-}$ mutants plotted closely with its predicted mean, and the measured mean for *Ephb2*$^{-/-}$; *Ephb3*$^{-/-}$ mutants also plotted in almost the same location as its predicted mean (Figure 3D). However, the measured mean for *Ephb1*$^{-/-}$; *Ephb3*$^{-/-}$ mutants had a statistically significantly larger PC1 compared to its predicted mean (signified by a colored arrow in Figure 3D), and this shift was similar in direction to that observed in *Ephb1* heterozygous and homozygous mutants (Figure 3A, Supplementary Table S4).

Overall, these results suggest that while specimens of most genotypes exhibited facial shapes that matched predictions of our additive genetic model, there are a few genotypes that deviated from additive genetic expectations. Of particular interest are the shape effects conferred by loss of *Ephb1* that were not fully explained by our simple models. *Ephb1*$^{+/-}$, *Ephb1*$^{-/-}$, and *Ephb1*$^{-/-}$; *Ephb3*$^{-/-}$ specimens had larger PC1 scores than predicted by both our simple additive and interaction models. The higher-than-expected PC1 scores for these genotypes were characterized by relative facial shape changes including a mediolaterally wider but dorsoventrally shorter face. However, homozygous loss of *Ephb1* appeared to have minimal effects when found in combination with homozygous loss of *Ephb2*, evidenced by *Ephb1*$^{-/-}$; *Ephb2*$^{-/-}$ mutants being similar in shape to *Ephb2*$^{-/-}$ mutants and not having the positive PC1 score divergence that is exhibited by other *Ephb1* genotypes. Further, facial dysmorphology was similar between *Ephb2*$^{-/-}$; *Ephb3*$^{-/-}$ mice and *Ephb1*$^{-/-}$; *Ephb2*$^{-/-}$; *Ephb3*$^{-/-}$ mice, providing additional support for genetic dominance of *Ephb2* effects over relatively weak *Ephb1* effects.

2.4 | Craniofacial size comparison

To determine whether loss of different *Ephb* alleles influences absolute measures of craniofacial size (rather than relative facial shape changes described in the PC plots above), we first compared total head volume for select genotypes, and then computed linear distances between select craniofacial landmarks (Figure 1B). We chose linear measurements that represented facial width at different positions across the face, a measure of facial length, as well as upper lip height. While the small within-genotype sample sizes and high shape variation for each genotype did not allow for effective pairwise statistical comparisons of landmark coordinate shape variables between specific genotypes, visually comparing multiple craniofacial size measures aided in determining if there were shifts in total head size or in the size of specific facial regions related to genotypic shape effects described above. For example, a relatively wide face within a shape analysis where all faces are scaled to a common size (as in our shape analysis above) can be generated by increased interorbital distance or by a decrease in size of other regions of the face, as both situations will make the distance between the orbits large relative to the rest of the face.

A nonstatistical comparison of overall head volume did not indicate a consistent effect on overall head size across mutations when compared to controls. However, specific *Ephb* receptor gene mutations were associated with distinct craniofacial size effects. *Ephb1*$^{+/-}$, *Ephb1*$^{-/-}$, and *Ephb1*$^{-/-}$; *Ephb3*$^{-/-}$ mutants were the most divergent and had smaller mean head volumes than controls (Figure 4A). In contrast, *Ephb2*$^{-/-}$ and *Ephb3*$^{-/-}$ single gene homozygotes and *Eph2*$^{-/-}$; *Ephb3*$^{-/-}$, and *Ephb1*$^{+/-}$; *Ephb2*$^{+/-}$; *Ephb3*$^{+/-}$ mutants also differed from controls by having larger mean head volumes (Figure 4A). These results indicate that overall growth and development of the head in E14.5 mice is impacted differently by specific *Ephb* receptor genotype combinations.

In addition to comparing overall head volume between *Ephb* receptor genotypes, we compared size in different regions of the face. We first calculated the linear correlation between facial size measures and head volume to determine how each measure scales with overall head size and then visually compared craniofacial measures between specific genotypes to look for differences in absolute facial size measures. Similar to head volume,

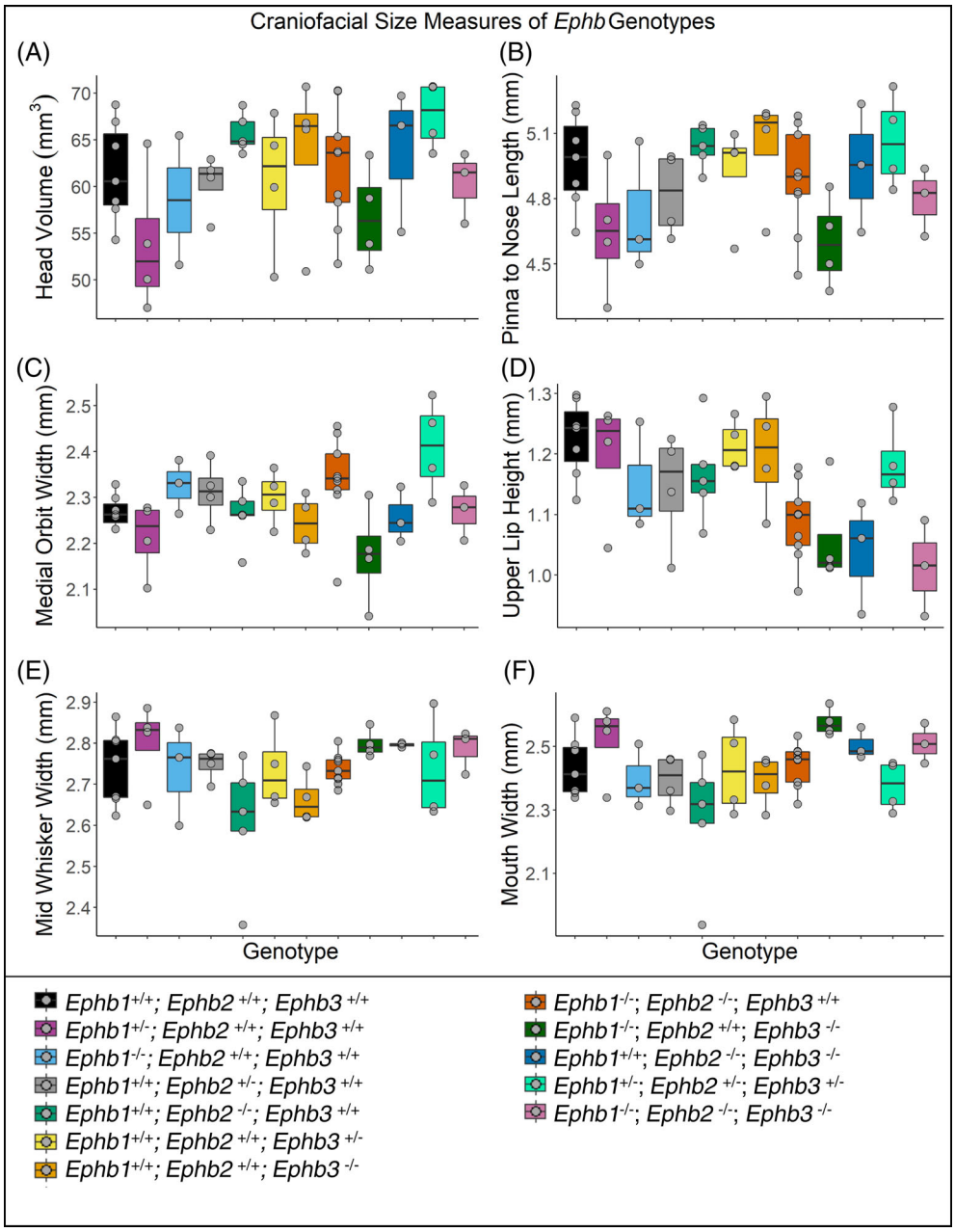

FIGURE 4 (A) Total craniofacial volume and (B-F) linear distances taken between measured 3D craniofacial landmarks for select *Ephb* mutant genotypes to examine allometric differences in craniofacial measures. For each boxplot, middle line represents the median value (50th percentile), while the lower and upper hinges represent the first and third quartiles (25th and 75th percentiles, respectively). Whiskers extend to the values 1.5 * distance between first and third quartiles (ie, inter-quartile range) from each hinge. Values beyond the whiskers are considered outliers and are plotted individually

TABLE 2 Linear regressions of linear facial measurements by total head volume

Linear model	Slope	Intercept	Adjusted R^2	F	*P*-value
Face length (FL) ~ Head volume	0.036	2.66	0.88	365.8	<.001
Medial orbit width (MO) ~ Head volume	0.0075	1.82	0.27	19.78	<.001
Upper lip height (LH) ~ Head volume	0.0060	0.77	0.14	9.406	.003
Mid whisker width (WW) ~ Head volume	−0.0076	3.20	0.24	17.72	<.001
Mouth width (MW) ~ Head volume	−0.0092	3.00	0.22	15.9	<.001

Note: Pinna to nose length (representing face length) has a strong, isometric relationship with head volume. Medial orbit width and upper lip height have weak, positive correlations with head volume, while mid-whisker width and mouth width both have weak, negative correlations with head volume.

we did not identify a consistent effect across genotypes for facial region size measures. Pinna to nose length (ie, face length) had a strong, isometric relationship with head volume (Table 2). Similar to head volume, mean face length was smallest in *Ephb1*$^{+/-}$, *Ephb1*$^{-/-}$, and *Ephb1*$^{-/-}$; *Ephb3*$^{-/-}$ mutants, and largest in *Ephb2*$^{-/-}$,

Ephb3$^{-/-}$, and *Ephb1*$^{+/-}$; *Ephb2*$^{+/-}$; *Ephb3*$^{+/-}$ mutants (Figure 4B). Medial orbit width and upper lip height had weak, positive correlations with head volume (Table 2). Interorbital distance was largest in *Ephb1*$^{-/-}$, *Ephb1*$^{-/-}$; *Ephb2*$^{-/-}$ and *Ephb1*$^{+/-}$; *Ephb2*$^{+/-}$; *Ephb3*$^{+/-}$ mutants compared to other genotypes (Figure 4C). Height of the upper lip was smallest in *Ephb1*$^{-/-}$; *Ephb2*$^{-/-}$; *Ephb3*$^{-/-}$ mutants as well as all double homozygous mutants, suggesting a shortened philtrum with homozygous loss of two or more *Ephb* receptor genes (Figure 4D). Mid-whisker width and mouth width both had weak, negative correlations across the genotypes measured (Table 2), such that specimens with larger heads tended to have narrower maxillary regions. These two measures were larger in *Ephb1*$^{+/-}$, *Ephb1*$^{-/-}$; *Ephb3*$^{-/-}$ and *Ephb2*$^{-/-}$; *Ephb3*$^{-/-}$, and *Ephb1*$^{-/-}$; *Ephb2*$^{-/-}$; *Ephb3*$^{-/-}$ mutants compared to controls (Figure 4E,F).

In summary, there were noticeable differences between *Ephb* mutants in some aspects of facial size as well as overall mean head volume. However, unlike the shape effects of *Ephb* gene mutations which appeared to be primarily linear in nature (discussed above), there was not a consistent size effect pattern identified across *Ephb* genotypes. For example, *Ephb1*$^{+/-}$, *Ephb1*$^{-/-}$, and *Ephb1*$^{-/-}$; *Ephb3*$^{-/-}$ mutants were most different in size from controls with overall smaller heads and wider and shorter faces, while *Ephb2*$^{-/-}$ and *Ephb3*$^{-/-}$ mutants had slightly larger heads with faces similar in length and width compared to controls. Shape results instead indicated that *Ephb2*$^{-/-}$ and *Ephb3*$^{-/-}$ mutants were more different from controls in craniofacial shape than *Ephb1* mutants. Size differences in *Ephb1*$^{+/-}$, *Ephb1*$^{-/-}$, and *Ephb1*$^{-/-}$; *Ephb3*$^{-/-}$ mutants may be related to the *Ephb1* nonadditive facial shape effect identified in our earlier shape analysis. Results of our size analyses also provided additional support for a dominant effect of *Ephb2* over *Ephb1* receptor gene mutations for some aspects of facial size. For example, compared to controls, interorbital distance was smaller in *Ephb1*$^{-/-}$; *Ephb3*$^{-/-}$ mutants, larger in *Ephb1*$^{-/-}$; *Ephb2*$^{-/-}$ mutants, and similar in size between *Ephb2*$^{-/-}$; *Ephb3*$^{-/-}$ and *Ephb1*$^{-/-}$; *Ephb2*$^{-/-}$; *Ephb3*$^{-/-}$ mutants. One unexpected result was the size effect associated with heterozygous loss of all three receptors. *Ephb1*$^{+/-}$; *Ephb2*$^{+/-}$; *Ephb3*$^{+/-}$ mutants had larger head volumes and facial measures than most genotypes but did not display the smaller upper lip height seen in all other mutants with homozygous loss of a combination of two or all three receptor genes. This suggests that heterozygosity for *Ephb1-3* may have different developmental effects on craniofacial size than homozygosity and that these size effects may be independent of shape effects.

3 | DISCUSSION

Determining how paralogous genes function to control craniofacial size and shape is a key part of understanding mammalian morphological diversity. Gene paralogs can have redundant or unique roles during facial development and may interact at the same developmental timepoint or region to determine facial morphology. Here, we identified specific additive and nonadditive effects of mutations in three *Ephb* receptor gene paralogs, which are expressed during early craniofacial development and help mediate normal head and facial morphogenesis through EPH/EPHRIN signaling.[14,19,20,25,26,31] *Ephb1-3* receptors have overlapping expression in the developing head and face of mice and are presumed to have similar downstream signaling capabilities.[14,18,20,28,31,32] Functional similarities between receptors in the same family are likely because they are the result of numerous gene duplications that occurred across the evolutionary history of vertebrates. However, over time, duplicate receptors diversify in their function to varying degrees. Ongoing work continues to improve our understanding of the redundancy and divergence of *Eph* receptor expression throughout development of the craniofacial complex and the rest of the body. Here, quantifying and describing the specific effects of each *Ephb* receptor paralog helped identify additive and nonadditive genetic effects associated with different combinations of allele mutations and the influence of each receptor on craniofacial morphology. Further, we identified potential regions of overlap between *Ephb1-3* receptor genes based on shared shape effects in mutants and determined how loss of more than one receptor gene influenced facial shape.

The E14.5 *Ephb1-3* allelic series that we analyzed here, including all 27 unique genotype combinations, is especially well suited to identify overall facial shape effects of heterozygous or homozygous loss of each *Ephb* receptor gene on its own, and to detect interaction effects between genes on facial morphology. We made several observations that imply both unique and redundant functions of these receptors on craniofacial size and shape. For example, this large number of genotypes enabled us to identify general similarities and differences in the additive shape effects between *Ephb2* and *Ephb3*, such as antero-inferior displacement of the ear pinnae and a shortened upper lip in *Ephb3* mutants that is not seen in *Ephb2* mutants. This suggests that *Ephb3* may be more important to lower face and ear development than *Ephb2*. We also identified a more severe dysmorphology associated with loss of both *Ephb2* and *Ephb3* receptors, which is consistent with previous work examining the phenotypic effects of *Ephb1-3* mutations that has described

more severe facial dysmorphology in *Ephb2*$^{-/-}$ and *Ephb3*$^{-/-}$ mutants compared to *Ephb1*$^{-/-}$ mutants.[14,31] A visual comparison of the shape changes exhibited in our sample of *Ephb* receptor mutants (Figure 2) with *Efnb1* male hemizygous (*Efnb1*$^{\Delta/Y}$) and *Efnb1* female heterozygous (*Efnb1*$^{+/\Delta}$) embryos[24] suggested similar changes exhibited across the face such as facial shortening, hypertelorism, and decreased lip height. However, homozygous loss of *Ephb1-3* did not lead to the severe phenotype seen in *Efnb1*$^{+/\Delta}$ mice, and facial shape changes in *Ephb2*$^{-/-}$ mutants were instead notably similar to *Efnb1*$^{\Delta/Y}$ embryos.[14] Further, mutants with loss of all three EPHB receptors still exhibited some degree of EPHRIN-B1 mediated cell segregation, which suggests that there may be other receptors interacting with EPHRIN-B1 during craniofacial development. Future work should examine other EPH receptors to determine how additional EPH/EPHRIN signaling influences craniofacial dysmorphology.

Our statistical models indicated that *Ephb1*, *Ephb2*, and *Ephb3* genotypes each had a statistically significant additive genetic influence on facial shape, and that *Ephb2* and *Ephb3* had the strongest effects on craniofacial morphology. The measured facial shapes of *Ephb2* and *Ephb3* mutants plotted closely to the facial shapes predicted by our additive model, indicating additive genetic effects associated with both receptors. Following predictions of an additive genetic model, the facial dysmorphologies of *Ephb2*$^{-/-}$ and *Ephb3*$^{-/-}$ mice appeared to be approximately twice as severe as dysmorphologies for *Ephb2*$^{+/-}$ and *Ephb3*$^{+/-}$ mice, respectively. However, while measured PC scores for both *Ephb2*$^{+/-}$ and *Ephb3*$^{+/-}$ mutant embryos plotted closely with their predicted PC scores, measured individuals also overlapped with controls, which may instead indicate a minor or no effect of heterozygosity on facial shape. In this case, our sample size does not allow us to distinguish between a minor heterozygous effect (as would be expected with a truly additive effect) and a threshold effect where heterozygotes have no appreciable dysmorphology. Future work and a larger sample can clarify this result.

Although each individual receptor contributed significantly to craniofacial shape, our statistical model did not identify significant pairwise interaction effects between any two receptor genes. A significant interaction effect between a pair of receptors would indicate that this combination of two receptor mutant alleles consistently leads to a phenotype that diverges from the additive model expectation in a certain way. As our statistical model did not indicate significant pairwise interactions, this either means that there were no interaction effects between pairs of alleles or that there were no consistent nonlinear pairwise interaction effects. This does not preclude nonadditive genetic interactions between certain pairs of alleles within certain genotypic contexts. Although a significant interaction effect between *Ephb1* and *Ephb2* was not identified in our statistical model, the *P*-value of this pairwise interaction effect is close to the 0.05 cutoff ($P = .075$), suggesting that this interaction effect might have reached significance with a larger sample size. This potential close to significant interaction would help explain the proposed interaction effect between EPHB1 and EPHB2 receptors that we describe below based on the comparison of model predictions and measured genotype-specific facial shape.

There was a significant nonadditive interaction identified when all three *Ephb* receptor genotypes were considered at once. Based on our visual assessment of measured and predicted PC scores across the sample, this interaction effect may indicate that the *Ephb1* genotype demonstrates a recessive nature when in the presence of both *Ephb2* and *Ephb3* mutations. *Ephb2*$^{-/-}$; *Ephb3*$^{-/-}$ mutants had facial shape and size measures that were consistent with the effects of an additive genetic model and appeared to have a more extreme phenotype than other genotypes. In fact, *Ephb2*$^{-/-}$; *Ephb3*$^{-/-}$ mutants were very similar in size and shape to *Ephb1*$^{-/-}$; *Ephb2*$^{-/-}$; *Ephb3*$^{-/-}$ mutants. Previous work has found that *Ephb2*$^{-/-}$; *Ephb3*$^{-/-}$ mutants approach the phenotype of *Efnb1*$^{\Delta/Y}$ *embryos*, and facial shape changes are in the direction of *Efnb1*$^{+/\Delta}$ embryos.[14] In agreement with other studies, our study supports EPHB2 and EPHB3 as being key receptors during craniofacial development in E14.5 mice.[14,19,28,31]

While the facial shapes of most genotypes were predicted well by the additive factors in our statistical model, a visual examination of the allelic series allowed us to identify a pattern that might indicate genotype-specific, nonadditive genetic interaction effects. The *Ephb1* genotype was identified as having a statistically significant additive effect on facial shape, although it is the weakest effect among the three receptors. In fact, predicted *Ephb1*$^{+/-}$ and *Ephb1*$^{-/-}$ mutant facial shapes were very similar to control specimen facial shape. This result is consistent with a previous study that described minimal effects of *Ephb1* on facial morphology paired with low *Ephb1* expression in the palate and the frontonasal prominence in early mouse development.[14] However, the measured facial shape means for *Ephb1*$^{+/-}$ and *Ephb1*$^{-/-}$ mutant specimens suggest more severe effects of *Ephb1* that are not explained by our statistical models. Specifically, *Ephb1*$^{+/-}$ and *Ephb1*$^{-/-}$ mutants usually had higher PC1 scores than their predicted means (Figure 3A). This unexpected position of *Ephb1* measured mean shape toward the positive end of PC1 was also seen in *Ephb1*$^{-/-}$; *Ephb3*$^{-/-}$ mutants, but not in *Ephb1*$^{-/-}$; *Ephb2*$^{-/-}$ mutants, suggesting that there was an effect of

Ephb1 in some, but not all, of the compound mutant genotypes. The lack of *Ephb1* influence on facial shape when found in combination with an *Ephb2* homozygous mutant genotype suggests an interaction between EPHB1 and EPHB2 receptors during normal craniofacial development, such that normal expression of *Ephb2* alleles combined with homozygous loss of the *Ephb1* receptor gene (ie, $Ephb1^{-/-}$, $Ephb1^{+/-}$, and $Ephb1^{-/-}$; $Ephb3^{-/-}$ mutants) led to facial dysmorphology not predicted by our additive genetic model. One possible explanation for these surprising findings is that EPHB1 can hetero-oligomerize with other EPHB receptors to confer distinct EPH/EPHRIN signaling outcomes.[33] Indeed, it has been previously demonstrated that expression of EPHB1 with EPHB6 led to the formation of a more stable complex and increased phosphorylation of EPHB6 in NIH3T3 cells; EPHB2 can also hetero-oligomerize with other EPH receptors in HEK293 cells to mediate distinct signaling outcome.[33,34] Though EPHB1 hetero-oligomerization with EPHB2 has not been specifically examined, if such interactions are important, EPHB1 loss might impact signaling in the presence of EPHB2, and not in its absence. Indeed, we observed that EPHB1 loss did not impact facial shape in the absence of EPHB2, but did affect mean head shape in its presence, suggesting that hetero-oligomerization of EPHB1 and EPHB2 might be one possible explanation for this effect. Future in vivo biochemical interrogation of the relevance of hetero-oligomerization will be needed to address this question.

Our analysis identified craniofacial size as having the strongest effect on facial shape in our allelic series of E14.5 mice. Comparisons of craniofacial size and shape across the allelic series identified a degree of independence between the combined influence of receptor alleles. While shape effects of *Ephb* gene mutations were primarily linear in nature, size effects did not exhibit a consistent pattern across genotypes. Although the mean shape dysmorphology of $Ephb1^{+/-}$; $Ephb2^{+/-}$; $Ephb3^{+/-}$ mutants was intermediate between controls and $Ephb1^{-/-}$; $Ephb2^{-/-}$; $Ephb3^{-/-}$ mutants, mean craniofacial size is largest in $Ephb1^{+/-}$; $Ephb2^{+/-}$; $Ephb3^{+/-}$ mice despite controls and $Ephb1^{-/-}$; $Ephb2^{-/-}$; $Ephb3^{-/-}$ mutants being similar in mean head volume. $Ephb1^{+/-}$; $Ephb2^{+/-}$; $Ephb3^{+/-}$ mutants also had the largest interorbital distance of the genotypes examined but were similar to controls (but larger than $Ephb1^{-/-}$; $Ephb2^{-/-}$; $Ephb3^{-/-}$ mutants) in the size of other facial regions. This indicates a strong size effect in $Ephb1^{+/-}$; $Ephb2^{+/-}$; $Ephb3^{+/-}$ mutants that should be further examined. In addition, the proposed *Ephb1* effect on facial shape may also be secondary to a reduced craniofacial size of some *Ephb1* mutants. $Ephb1^{+/-}$, $Ephb1^{-/-}$, and $Ephb1^{-/-}$; $Ephb3^{-/-}$ mutants were most different in size from controls, with an overall smaller head and face but wider mid-whisker region and mouth. Further, $Ephb1^{-/-}$ mutants had a larger interorbital distance than controls. *Ephb1* gene mutations may reduce the overall size of E14.5 embryos, which then led to a different shape than predicted along PC1.

Although our size analysis compared craniofacial size across genotypes, potential size differences might also be measured in postcranial regions (eg, upper and lower limb length, trunk length) and other head tissues to determine if the *Ephb1* effect identified here is limited to certain craniofacial tissues or if it leads to systemic growth effects throughout the body. For example, changes in craniofacial size have been proposed to reflect differences in brain or neurocranial morphology through shared origins of tissues, interactions between adjacent tissues and shared signaling between regions.[14,35-38] The brain provides a platform for the developing face, and an increase in brain growth can lead to changes in the positioning and size of facial tissues.[35] As EPHB1 has low levels of expression in craniofacial mesenchyme and is more involved in cell segregation in the brain,[14] a decrease in overall brain size may explain why *Ephb1* mutants in our sample have smaller heads and facial sizes than other receptor mutants. However, Niethamer and colleagues[14] determined that facial dysmorphogenesis in *Efnb1* mutant embryos was not primarily caused by differences in brain morphology. Instead, facial shape was primarily altered by segregation of facial tissues derived from neural crest cells (NCCs), resulting in *Efnb1* mosaicism in the face. Therefore, it is unclear whether variation in facial size across our genotypes involves changes to brain growth or facial mesoderm growth. We did not have the postcranial data to determine whether craniofacial size or shape differences are the result of differences in overall embryo size. While we did not find size changes related specifically to the number of mutations present (ie, more mutations did not always lead to smaller heads), it is possible that craniofacial changes related to *Ephb* mutations are related to a more widespread developmental delay influencing both head and body size. Unfortunately, this hypothesis cannot be tested with the current sample.

Describing the contribution of individual *Ephb* mutant genotypes during facial morphogenesis substantially improves our understanding of their relative importance in producing normal and disease phenotypes, such as hypertelorism and frontonasal dysplasia observed in CFNS.[14,15,19,22,31] EPHB1-3 interact biochemically with EPHRIN-B1, and these findings have significance for understanding mechanisms underlying CFNS pathogenesis. Specifically, our results suggest that in vivo, EPHB2 and EPHB3 may be the main EPHRIN-B1 receptors, whereas the role of EPHB1 in craniofacial morphogenesis may function through EPHB2 or EPHB3. Several other

aspects of EPH/EPHRIN signaling biology might underlie the combined additive and nonadditive effects that we identify here. First, in addition to being receptors for EPHRIN-B1, EPHB1-3 also bind with similar affinity to EPHRIN-B2 and EPHRIN-B3,[19] and EPHB2 is also a receptor for A-type EPHRINs including EPHRIN-A5.[39] Though the role of EPHB1 remains incompletely understood, comparing phenotypes resulting from EPHRIN-B1 loss with EPHB2; EPHB3 compound homozygous mutants strongly supports that EPHB2 and EPHB3 mainly partner with EPHRIN-B1 in craniofacial morphogenesis.

Our detailed analysis of the morphologies across this *Ephb* allelic series clarifies the specific roles of EPHB receptors as critical components of EPH/EPHRIN signaling during normal facial development. Determining whether *Ephb* genes exhibit additive or nonadditive genetic effects also indicates the likely presence of incompletely understood signaling interactions between EPHB receptors that bind to the same EPHRIN ligands. Deeper mechanistic interrogation of these receptor interactions will improve our understanding of the combinatorial effect of allelic variation across multiple receptor genes on normal processes of facial development and how these genes might underly CFNS-like dysmorphologies in humans. A deeper understanding of these genetic interactions may ultimately aid in efforts to predict disease morphology from genotype and may aid in efforts to mitigate or treat the effects of the CFNS mutations.

4 | EXPERIMENTAL PROCEDURES

4.1 | Materials

4.1.1 | Ethics statement

All animal experiments were performed in accordance with the protocols of the University of California, San Francisco Institutional Animal Care and Use Committee under approval number AN182040-01. Mice were socially housed under a 12-hour light-dark cycle with ad libitum food and water. Additional enrichment was provided if single housing was required for breeding purposes. Mice were euthanized by CO_2 inhalation followed by cervical dislocation when necessary.

4.1.2 | Mouse lines and generation of EPHB receptor compound mutants

All alleles used for the experiments herein have been previously described.[14] All mice were maintained and backcrossed on a congenic C57BL/6J genetic background: *Ephb1*$^{-}$, MGI: 2677305[40]; *Ephb2*$^{-}$, MGI: 2149765[41]; *Ephb3*$^{-}$, MGI: 2149669.[28] E14.5 embryos with various combinations of *Ephb1-3* allele mutations were collected from crosses of male and female mice carrying differing numbers of *Ephb1-3* mutant receptor alleles (Table 3). This *Ephb* allelic series was originally generated as a comparative sample to E11.5-E14.5 *Efnb1* mutants.[14] E14.5 was the latest age within the *Efnb1* range and was chosen for the *Ephb* allelic series embryo collection because they had the strongest dysmorphology in the original sample.

4.1.3 | Morphometrics data acquisition

Embryos were fixed and stored in a mixture of 4% paraformaldehyde (PFA) and 5% glutaraldehyde in PBS. After approximately an hour soaking in Cysto-Conray II

TABLE 3 Sample sizes for allelic series of *Ephb* genotypes

Genotype	Sample size
Ephb1$^{+/+}$; *Ephb2*$^{+/+}$; *Ephb3*$^{+/+}$ (control)	7
Ephb1$^{+/-}$	4
Ephb1$^{-/-}$	3
Ephb2$^{+/-}$	4
Ephb2$^{-/-}$	5
Ephb3$^{+/-}$	4
Ephb3$^{-/-}$	4
Ephb1$^{+/-}$; *Ephb2*$^{+/-}$	4
Ephb1$^{-/-}$; *Ephb2*$^{+/-}$	7
Ephb1$^{+/-}$; *Ephb2*$^{-/-}$	5
Ephb1$^{-/-}$; *Ephb2*$^{-/-}$	9
Ephb1$^{+/-}$; *Ephb3*$^{+/-}$	5
Ephb1$^{-/-}$; *Ephb3*$^{+/-}$	4
Ephb1$^{+/-}$; *Ephb3*$^{-/-}$	3
Ephb1$^{-/-}$; *Ephb3*$^{-/-}$	4
Ephb2$^{+/-}$; *Ephb3*$^{+/-}$	6
Ephb2$^{-/-}$; *Ephb3*$^{+/-}$	5
Ephb2$^{+/-}$; *Ephb3*$^{-/-}$	2
Ephb2$^{-/-}$; *Ephb3*$^{-/-}$	3
Ephb1$^{+/-}$; *Ephb2*$^{+/-}$; *Ephb3*$^{+/-}$	4
Ephb1$^{-/-}$; *Ephb2*$^{+/-}$; *Ephb3*$^{+/-}$	4
Ephb1$^{+/-}$; *Ephb2*$^{-/-}$; *Ephb3*$^{+/-}$	5
Ephb1$^{+/-}$; *Ephb2*$^{+/-}$; *Ephb3*$^{-/-}$	3
Ephb1$^{-/-}$; *Ephb2*$^{-/-}$; *Ephb3*$^{+/-}$	6
Ephb1$^{-/-}$; *Ephb2*$^{+/-}$; *Ephb3*$^{-/-}$	4
Ephb1$^{+/-}$; *Ephb2*$^{-/-}$; *Ephb3*$^{-/-}$	5
Ephb1$^{-/-}$; *Ephb2*$^{-/-}$; *Ephb3*$^{-/-}$	3

(Liebel-Flarsheim Canada), micro-computed tomography (μCT) images of embryo heads were acquired with a Scanco μCT35 at the University of Calgary or a Scanco μCT40 at Stony Brook University with 45 kV/177 μA for images of 0.012 mm^3 voxel size. All facial landmarks were collected on minimum threshold-based ectodermal surfaces (downsampled ×2) from the μCT images in Amira (Thermo-Fisher) by the same observer (Figure 1A). Landmarks used in morphometric analyses were previously defined (Supplementary Table S5).[14]

To examine the relationship between genotype and craniofacial size, specific linear distances between 3D facial landmarks were calculated to represent different aspects of facial morphology (Figure 1B). These measurements were calculated using the raw landmarks before they were scaled, rotated, and translated for the generalized Procrustes analysis (GPA) (described below) and therefore capture absolute measures of craniofacial size. Craniofacial size was also captured as total head volume using ectodermal surfaces. Surfaces were cropped with a standardized procedure using the "Trim to Plane" tool in Geomagic Studio 2012 (Geomagic, Morrisville, North Carolina). Points were placed under the left and right inferior ear pinnae and the mid-sagittal point of the mandible, the plane was set to connect these three points, and all material inferior to this plane was removed. The resulting opening at the base of the head was filled with a flat surface using the "Fill All Holes" tool to create an enclosed surface which is necessary to calculate head volume in Geomagic. Within the Procrustes ANOVA analyses, facial size is quantified as the centroid size of all facial landmarks, as estimated during the Procrustes superimposition procedure described below.

4.2 | Methods

A flowchart of all methods and materials is represented in Figure 5.

4.2.1 | GPA and data preparation

We performed a geometric morphometric analysis of facial landmarks using *geomorph*[42] and RRPP[43] libraries in R Statistical software.[44] We first performed a GPA to translate, scale, and rotate landmark coordinates to align each specimen's landmark coordinates.[45] Further analyses were run with the symmetric component of specimen landmark coordinate variation, as we assumed that most bilateral shape differences between the left and right sides of a specimen's face are due to random effects associated with developmental noise and tissue fixation.[46] Thus, symmetrized landmark coordinate data are interpreted to better represent the typical genotype effects on facial shape while minimizing random variation from stochastic developmental processes and minor tissue fixation artifacts.[47,48]

To identify significant differences in landmark coordinates between genotypes, we compared facial shape coordinates of each mutant genotype with the variation in facial shape coordinates in control specimens. We estimated the 95% confidence interval of control genotype facial shape variation using the distribution of mean control specimen shapes generated across 1000 bootstrapped permutations of the control specimen sample (seven specimens, sampled with replacement each time). We then measured the Procrustes distances between each mutant genotype mean shape and the measured control specimen mean shape. If the distance calculated for a mutant genotype was longer than the 95% CI of control specimen shape variation, this indicated a significant difference in facial shape between that mutant genotype and control specimens (Supplementary Table S2).

4.2.2 | Procrustes ANOVA

We ran two Procrustes analysis of variance (ANOVA) models to quantify the relative amount of facial shape variance that can be attributed each *Ephb* receptor gene and to facial size, as well as potential interaction effects between multiple receptor genotypes.[42] This analysis uses 3D symmetrized landmark coordinates as the response variable, and size (numeric: centroid size) and genotype (separate numeric factors: 0, 1, 2 mutant alleles for *Ephb1*, *Ephb2*, and *Ephb3*) as independent variables. Sum-of-squared Procrustes distances were used to estimate sum of squares (SS). The amount of shape variation associated with each factor was then quantified and compared to a null model using resampling permutation.[42,49] The relative impacts of facial size and of each *Ephb* gene on facial shape across the entire sample are quantified as the effect size (*Z*-score), while the amount of facial shape variation attributable to facial size and of each *Ephb* receptor gene are described using R-squared (Rsq) values. We ran one model incorporating additive effects (coords∼Csize+*Ephb1* + *Ephb2* + *Ephb3*) and one model incorporating interaction effects (coords∼Csize + *Ephb1* * *Ephb2* * *Ephb3*) in the independent genotype variables. While both models incorporate the same information about size and genotype factors, the interaction model incorporates additional variables that represent nonadditive interactions between different *Ephb* receptor genotypes in producing facial shape.

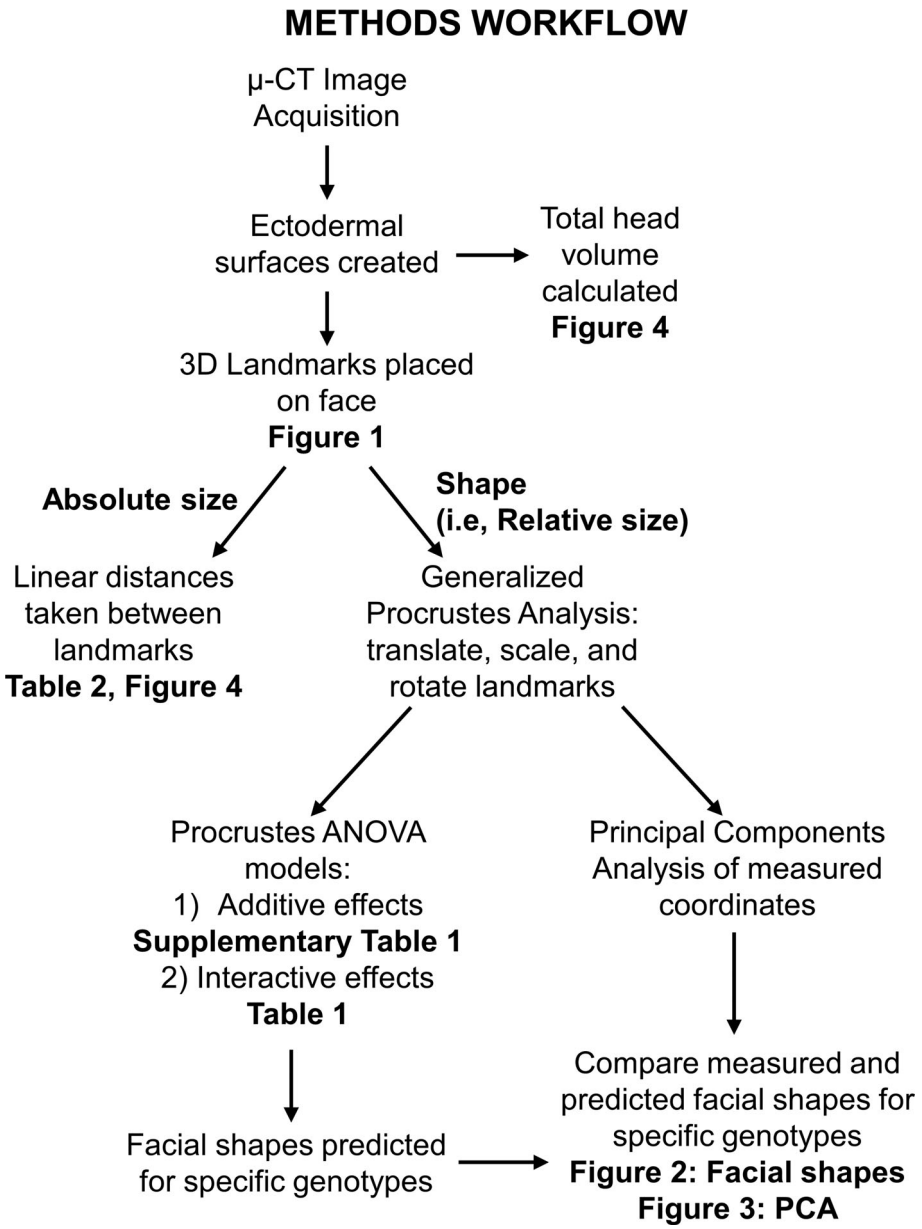

FIGURE 5 Flowchart representation of methods and analyses performed

These models were utilized in subsequent analyses to predict craniofacial shapes for specific genotypes based on calculated additive or interaction effects across the allelic series (Figure 2). While information from the models takes into account the relative influence of each receptor based on all combinations of alleles, we chose specific genotypes to analyze in more detail: controls (*Ephb1*$^{+/+}$; *Ephb2*$^{+/+}$; *Ephb3*$^{+/+}$), single gene heterozygotes (*Ephb1*$^{+/-}$, *Ephb2*$^{+/-}$, or *Ephb3*$^{+/-}$), single-gene homozygotes (*Ephb1*$^{-/-}$, *Ephb2*$^{-/-}$, or *Ephb3*$^{-/-}$), double-gene homozygotes (*Ephb1*$^{-/-}$; *Ephb2*$^{-/-}$, *Ephb1*$^{-/-}$; *Ephb3*$^{-/-}$, or *Ephb2*$^{-/-}$; *Ephb3*$^{-/-}$), triple gene heterozygotes (*Ephb1*$^{+/-}$; *Ephb2*$^{+/-}$; *Ephb3*$^{+/-}$), and triple gene homozygotes (*Ephb1*$^{-/-}$; *Ephb2*$^{-/-}$; *Ephb3*$^{-/-}$).

4.2.3 | Predicted and measured principal components analysis

We utilized the fitted values and associated covariates from the additive and interaction Procrustes ANOVA models to predict average facial shape landmark coordinates for each genotype in the allelic series. Predicted landmarks were estimated from linear models that consider the relative influence of each receptor allele across the entire sample of specimens rather than only for specific genotypes. This method was chosen because it allows us to effectively summarize genotypic effects across a large number of genotypes that would not be possible with a series of pairwise comparisons between genotypes. Further, comparing shape effects from both

an additive and an interaction model enabled us to compare the shape effects predicted for a simpler additive model with one that also incorporates interaction between different *Ephb* alleles to determine how nonadditive effects play an additional role in facial morphology. Visualizing predicted facial shapes allowed for comparison of overall genotypic effects to determine the additive or interaction effects of specific *Ephb* receptor genes. We plotted predicted facial shape coordinates to visualize overall trends in *Ephb* gene mutation shape effects for single, double, and triple gene homozygous mutants compared to controls.

To further compare general patterns of genotype effects, we ran a principal components analysis (PCA) on the previously aligned, symmetrized landmark coordinates for measured specimens and calculated the mean principal components (PC) scores for genotypes of interest.[42] These mean scores represent the average facial shapes of genotypes as measured directly from our landmarks. The associated PC axes represent the major axes of facial shape covariation in our measured sample. We then projected the additive and interaction model predicted facial shapes for specific genotypes onto these PC axes to determine whether our measured sample means aligned closely with the predicted genotype means (Figure 3).

We compared the mean measured facial shapes with predicted facial shapes to determine whether the effects of individual receptor alleles follow general trends predicted by an additive model or one that also incorporates interaction effects. We also looked for any patterns of systematic divergence of measured facial shapes from model predicted facial shapes across genotypes. If measured PC scores aligned closely with predicted additive model PC scores for the genotypes examined, *Ephb* receptor genes likely have additive genetic influence on craniofacial morphology. If there are significant differences between the average facial shape of measured specimens and the predictions of both our additive and interaction models, *Ephb* receptor genes may interact nonadditively in ways that are not consistent across all combinatorial genotypes in our sample. For example, this may indicate genetic dominance of one receptor gene over another when they are found in certain combinations.

To identify significant differences between our predicted and measured PC scores, we bootstrapped single genotype sample PC scores with replacement to generate a 95% confidence interval (CI) of the mean of measured samples from that genotype. This process was completed first for controls and then for specific mutant genotypes. If predicted means fell outside the measured mean CI, then there is a significant difference between the average measured and predicted facial shapes of a given genotype ($\alpha = .05$). This would indicate that the measured mutant sample instead exhibits a facial shape that is not explained by our predictive ANOVA model (Results in Supplementary Table S4).

ACKNOWLEDGEMENTS

The authors thank the Functional Morphology Lab and Percival Lab at Stony Brook University for comments on early drafts of results. The authors also thank Benedikt Hallgrímsson for the use of his μCT systems at the University of Calgary Cumming School of Medicine and Isabel Mormile for collecting μCT images at Stony Brook University. Sources of funding include NIH/NIDCR R01-DE023337 and startup funds to Christopher J. Perciva from Stony Brook University.

AUTHOR CONTRIBUTIONS

Sarah Thomas Mincer: Formal analysis (lead); investigation (equal); methodology (equal); visualization (lead); writing – original draft (lead); writing – review and editing (equal). **Terren K. Niethamer:** Data curation (equal); project administration (equal); writing – review and editing (equal). **Teng Teng:** Data curation (equal); project administration (equal); writing – review and editing (supporting). **Jeffrey O Bush:** Conceptualization (equal); data curation (equal); funding acquisition (lead); investigation (equal); project administration (equal); writing – review and editing (equal). **Christopher J Percival:** Conceptualization (equal); data curation (equal); formal analysis (equal); funding acquisition (equal); investigation (equal); methodology (equal); supervision (lead); writing – original draft (equal); writing – review and editing (equal).

CONFLICT OF INTEREST

The authors have no conflict of interest, financial or otherwise.

DATA AVAILABILITY STATEMENT

All relevant data are provided within the manuscript and accompanying Supplementary Information files.

ORCID

Sarah T. Mincer https://orcid.org/0000-0003-2275-7971

REFERENCES

1. Henikoff S, Greene EA, Pietrokovski S, Bork P, Attwood TK, Hood L. Gene families: the taxonomy of protein paralogs and chimeras. *Science*. 1997;278(5338):609-614.
2. Greer JM, Puetz J, Thomas KR, Capecchi MR. Maintenance of functional equivalence during paralogous Hox gene evolution. *Nature*. 2000;403(6770):661-665.
3. Massingham T, Davies L, Lio P. Analysing gene function after duplication. *Bioessays*. 2001;23(10):873-876.
4. Pollock RA, Sreenath T, Ngo L, Bieberich CJ. Gain of function mutations for paralogous Hox genes: implications for the

evolution of Hox gene function. *Proc Natl Acad Sci*. 1995; 92(10):4492-4496.
5. Mellott DO, Burke RD. The molecular phylogeny of eph receptors and ephrin ligands. *BMC Cell Biol*. 2008;9(1):1-8.
6. Dandage R, Landry CR. Paralog dependency indirectly affects the robustness of human cells. *Mol Syst Biol*. 2019; 15(9):e8871.
7. Diss G, Ascencio D, DeLuna A, Landry CR. Molecular mechanisms of paralogous compensation and the robustness of cellular networks. *J Exp Zool B Mol Dev Evol*. 2014;322(7): 488-499.
8. Pickett FB, Meeks-Wagner DR. Seeing double: appreciating genetic redundancy. *Plant Cell*. 1995;7(9):1347-1356.
9. Burke AC, Nelson CE, Morgan BA, Tabin C. Hox genes and the evolution of vertebrate axial morphology. *Development*. 1995;121(2):333-346.
10. Casaca A, Santos AC, Mallo M. Controlling Hox gene expression and activity to build the vertebrate axial skeleton. *Dev Dyn*. 2014;243(1):24-36.
11. Di-Poi N, Montoya-Burgos JI, Miller H, Pourquié O, Milinkovitch MC, Duboule D. Changes in Hox genes' structure and function during the evolution of the squamate body plan. *Nature*. 2010;464(7285):99-103.
12. Mallo M, Wellik DM, Deschamps J. Hox genes and regional patterning of the vertebrate body plan. *Dev Biol*. 2010;344(1): 7-15.
13. Diss G, Gagnon-Arsenault I, Dion-Coté A-M, et al. Gene duplication can impart fragility, not robustness, in the yeast protein interaction network. *Science*. 2017;355(6325):630-634.
14. Niethamer TK, Teng T, Franco M, Du YX, Percival CJ, Bush JO. Aberrant cell segregation in the craniofacial primordium and the emergence of facial dysmorphology in craniofrontonasal syndrome. *PLoS Genet*. 2020;16(2):e1008300.
15. Twigg SR, Kan R, Babbs C, et al. Mutations of ephrin-B1 (EFNB1), a marker of tissue boundary formation, cause craniofrontonasal syndrome. *Proc Natl Acad Sci*. 2004;101(23): 8652-8657.
16. Van Den Elzen M, Twigg S, Goos J, et al. Phenotypes of craniofrontonasal syndrome in patients with a pathogenic mutation in EFNB1. *Eur J Hum Genet*. 2014;22(8):995-1001.
17. Wieland I, Jakubiczka S, Muschke P, et al. Mutations of the ephrin-B1 gene cause craniofrontonasal syndrome. *Am J Hum Genet*. 2004;74(6):1209-1215.
18. Bush JO, Soriano P. Ephrin-B1 forward signaling regulates craniofacial morphogenesis by controlling cell proliferation across Eph–ephrin boundaries. *Genes Dev*. 2010;24(18):2068-2080.
19. Blits-Huizinga CT, Nelersa CM, Malhotra A, Liebl DJ. Ephrins and their receptors: binding versus biology. *IUBMB Life*. 2004; 56(5):257-265.
20. Kullander K, Klein R. Mechanisms and functions of Eph and ephrin signalling. *Nat Rev Mol Cell Biol*. 2002;3(7): 475-486.
21. Fagotto F, Winklbauer R, Rohani N. Ephrin-Eph signaling in embryonic tissue separation. *Cell Adh Migr*. 2014;8(4):308-326.
22. Kania A, Klein R. Mechanisms of ephrin–Eph signalling in development, physiology and disease. *Nat Rev Mol Cell Biol*. 2016;17(4):240-256.
23. Klein R, Kania A. Ephrin signalling in the developing nervous system. *Curr Opin Neurobiol*. 2014;27:16-24.
24. Niethamer TK, Bush JO. Getting direction (s): the Eph/ephrin signaling system in cell positioning. *Dev Biol*. 2019;447(1): 42-57.
25. Pasquale EB. Eph receptor signalling casts a wide net on cell behaviour. *Nat Rev Mol Cell Biol*. 2005;6(6):462-475.
26. Wilkinson DG. Multiple roles of EPH receptors and ephrins in neural development. *Nat Rev Neurosci*. 2001;2(3):155-164.
27. Wieacker P, Wieland I. Clinical and genetic aspects of craniofrontonasal syndrome: towards resolving a genetic paradox. *Mol Genet Metab*. 2005;86(1–2):110-116.
28. Orioli D, Henkemeyer M, Lemke G, Klein R, Pawson T. Sek4 and Nuk receptors cooperate in guidance of commissural axons and in palate formation. *EMBO J*. 1996;15(22):6035-6049.
29. Wei W, Wang H, Ji S. Paradoxes of the EphB1 receptor in malignant brain tumors. *Cancer Cell Int*. 2017;17(1):1-10.
30. Davy A, Bush JO, Soriano P. Inhibition of gap junction communication at ectopic Eph/ephrin boundaries underlies craniofrontonasal syndrome. *PLoS Biol*. 2006;4(10):e315.
31. Risley M, Garrod D, Henkemeyer M, McLean W. EphB2 and EphB3 forward signalling are required for palate development. *Mech Dev*. 2009;126(3–4):230-239.
32. Xavier GM, Miletich I, Cobourne MT. Ephrin ligands and Eph receptors show regionally restricted expression in the developing palate and tongue. *Front Physiol*. 2016;7:60.
33. Janes PW, Griesshaber B, Atapattu L, et al. Eph receptor function is modulated by heterooligomerization of a and B type Eph receptors. *J Cell Biol*. 2011;195(6):1033-1045.
34. Freywald A, Sharfe N, Roifman CM. The kinase-null EphB6 receptor undergoes transphosphorylation in a complex with EphB1. *J Biol Chem*. 2002;277(6):3823-3828.
35. Marcucio R, Hallgrimsson B, Young NM. Facial morphogenesis: physical and molecular interactions between the brain and the face. *Curr Top Dev Biol*. 2015;115:299-320.
36. Marcucio RS, Cordero DR, Hu D, Helms JA. Molecular interactions coordinating the development of the forebrain and face. *Dev Biol*. 2005;284(1):48-61.
37. Marcucio RS, Young NM, Hu D, Hallgrimsson B. Mechanisms that underlie co-variation of the brain and face. *Genesis*. 2011; 49(4):177-189.
38. Parsons TE, Schmidt EJ, Boughner JC, Jamniczky HA, Marcucio RS, Hallgrímsson B. Epigenetic integration of the developing brain and face. *Dev Dyn*. 2011;240(10):2233-2244.
39. Himanen J-P, Chumley MJ, Lackmann M, et al. Repelling class discrimination: ephrin-A5 binds to and activates EphB2 receptor signaling. *Nat Neurosci*. 2004;7(5):501-509.
40. Williams SE, Mann F, Erskine L, et al. Ephrin-B2 and EphB1 mediate retinal axon divergence at the optic chiasm. *Neuron*. 2003;39(6):919-935.
41. Henkemeyer M, Orioli D, Henderson JT, et al. Nuk controls pathfinding of commissural axons in the mammalian central nervous system. *Cell*. 1996;86(1):35-46.
42. Adams DC, Collyer ML, Kaliontzopoulou A. geomorph: Geometric Morphometric Analyses of 2D/3D Landmark Data Version 3.3.1. 2020.
43. Collyer ML, Adams DC. RRPP: an r package for fitting linear models to high-dimensional data using residual randomization. *Methods Ecol Evol*. 2018;9(7):1772-1779.
44. R Core Team. R. *A Language and Environment for Statistical Computing*. Vienna, Austria; 2020.

45. Bookstein FL. Morphometric tools for landmark data. *Geometry and Biology*. Cambridge, England, UK: Cambridge University Press; 1997.
46. Palmer AR, Strobeck C. Fluctuating asymmetry: measurement, analysis, patterns. *Ann Rev Ecol Syst*. 1986;17:391-421.
47. Mardia KV, Bookstein FL, Moreton IJ. Statistical assessment of bilateral symmetry of shapes. *Biometrika*. 2000;285-300: 285-300.
48. Klingenberg CP, Barluenga M, Meyer A. Shape analysis of symmetric structures: quantifying variation among individuals and asymmetry. *Evolution*. 2002;56(10):1909-1920.
49. Goodall C. Procrustes methods in the statistical analysis of shape. *J Roy Stat Soc Ser B*. 1991;53(2):285-321.

SUPPORTING INFORMATION

Additional supporting information may be found in the online version of the article at the publisher's website.

How to cite this article: Mincer ST, Niethamer TK, Teng T, Bush JO, Percival CJ. Investigating the effects of compound paralogous EPHB receptor mutations on mouse facial development. *Developmental Dynamics*. 2022;1-18. doi:10.1002/dvdy.454